

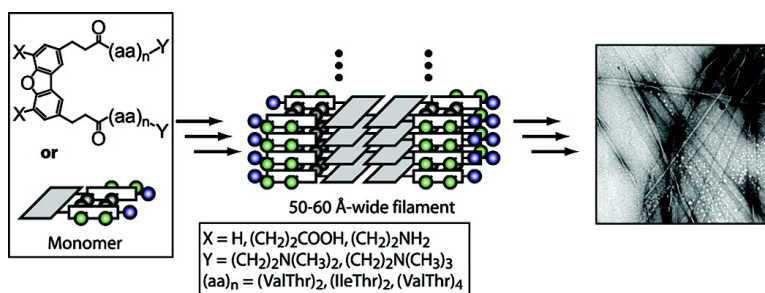
Article

## Controlling the Morphology of Cross $\beta$ -Sheet Assemblies by Rational Design

Songpon Deechongkit, Evan T. Powers, Shu-Li You, and Jeffery W. Kelly

*J. Am. Chem. Soc.*, **2005**, 127 (23), 8562-8570 • DOI: 10.1021/ja050558c • Publication Date (Web): 17 May 2005

Downloaded from <http://pubs.acs.org> on March 25, 2009



### More About This Article

Additional resources and features associated with this article are available within the HTML version:

- Supporting Information
- Links to the 2 articles that cite this article, as of the time of this article download
- Access to high resolution figures
- Links to articles and content related to this article
- Copyright permission to reproduce figures and/or text from this article

[View the Full Text HTML](#)

## Controlling the Morphology of Cross $\beta$ -Sheet Assemblies by Rational Design

Songpon Deechongkit, Evan T. Powers, Shu-Li You, and Jeffery W. Kelly\*

Contribution from the Department of Chemistry and The Skaggs Institute for Chemical Biology, The Scripps Research Institute, La Jolla, California 92037

Received January 27, 2005; E-mail: jkelly@scripps.edu

**Abstract:** Low molecular weight peptidomimetics with simple amphiphilic sequences can help to elucidate the structures of cross  $\beta$ -sheet assemblies, such as amyloid fibrils. The peptidomimetics described herein comprise a dibenzofuran template, two peptide strands made up of alternating hydrophilic and hydrophobic residues, and carboxyl termini, each of which can be varied to probe the structural requirements for  $\beta$ -sheet self-assembly processes. The dibenzofuran template positions the strands approximately 10 Å apart, allowing corresponding hydrophobic side chains in the strands to pack into a collapsed U-shaped structure. This conformation is stabilized by hydrophobic interactions, not intramolecular hydrogen bonds. Intermolecular stacking of the collapsed peptidomimetics, enabled by intermolecular hydrogen bonding and hydrophobic interactions, affords 25–27 Å wide protofilaments having a cross  $\beta$ -sheet structure. Association of protofilaments, mediated by the dibenzofuran substructures and driven by the hydrophobic effect, affords 50–60 Å wide filaments. These widths can be controlled by changing the length of the peptide strands. Further assembly of the filaments into fibrils or ribbons can be controlled by modification of the template, C-terminus, and buffer ion composition.

### Introduction

Many peptides and proteins form  $\beta$ -sheet-rich fibrillar aggregates. This phenomenon has attracted the attention of scientists from many fields because such assemblies both enable biological function and appear to cause pathology.<sup>1</sup> For example, the formation of fibrillar cross  $\beta$ -sheet assemblies results in functional materials, such as chorion, which is the main component of silk moth eggshells,<sup>2</sup> or curli fibrils, which are used by *Escherichia coli* (*E. coli*) in the colonization of surfaces.<sup>3</sup> In contrast, the misassembly of peptides or proteins can lead to cross  $\beta$ -sheet assemblies known as amyloid, the process of amyloidogenesis being implicated as the cause of several neurodegenerative diseases, including familial amyloid polyneuropathy and Alzheimer's disease.<sup>4–7</sup> Many authors have written about the potential use of ordered peptide assemblies as materials,<sup>8–30</sup> with suggested applications ranging from

responsive gels<sup>16,19,22,23</sup> and scaffolds for tissue regeneration<sup>26,28</sup> to substrates for crystal growth.<sup>21</sup> Exploiting the potential of  $\beta$ -sheet-based peptide assemblies requires an understanding of their internal structures that is detailed enough to allow rational

- (1) Huff, M. E.; Balch, W. E.; Kelly, J. W. *Curr. Opin. Struct. Biol.* **2003**, *13*, 674–682.
- (2) Iconomidou, V. A.; Vriend, G.; Hamodrakas, S. J. *FEBS Lett.* **2000**, *479*, 141–145.
- (3) Chapman, M. R.; Robinson, L. S.; Pinkner, J. S.; Roth, R.; Heuser, J.; Hammar, M.; Normark, S.; Hultgren, S. J. *Science* **2002**, *295*, 851–855.
- (4) Sipe, J. D. *Crit. Rev. Clin. Lab. Sci.* **1994**, *31*, 325–354.
- (5) Sipe, J. D.; Cohen, A. S. *J. Struct. Biol.* **2000**, *130*, 88–98.
- (6) Kelly, J. W. *Curr. Opin. Struct. Biol.* **1996**, *6*, 11–17.
- (7) Selkoe, D. J. *Nature* **2003**, *426*, 900–904.
- (8) Krejchí, M. T.; Atkins, E. D.; Waddon, A. J.; Fournier, M. J.; Mason, T. L.; Tirrell, D. A. *Science* **1994**, *265*, 1427–1432.
- (9) Winningham, M. J.; Sogah, D. Y. *Macromolecules* **1997**, *30*, 862–876.
- (10) Yamada, N.; Ariga, K.; Naito, M.; Matsubara, K.; Koyama, E. *J. Am. Chem. Soc.* **1998**, *120*, 12192–12199.
- (11) MacPhee, C. E.; Dobson, C. M. *J. Am. Chem. Soc.* **2000**, *122*, 12707–12713.
- (12) Lopez De La Paz, M.; Goldie, K.; Zurdo, J.; Lacroix, E.; Dobson, C. M.; Hoenger, A.; Serrano, L. *Proc. Natl. Acad. Sci. U.S.A.* **2002**, *99*, 16052–16057.
- (13) Moses, J. P.; Satheeshkumar, K. S.; Murali, J.; Alli, D.; Jayakumar, R. *Langmuir* **2003**, *19*, 3413–3418.
- (14) Sagis, L. M. C.; Veerman, C.; van der Linden, E. *Langmuir* **2004**, *20*, 924–927.
- (15) Matsumura, S.; Uemura, S.; Mihara, H. *Chem.–Eur. J.* **2004**, *10*, 2789–2794.
- (16) Aggeli, A.; Bell, M.; Boden, N.; Keen, J. N.; Knowles, P. F.; McLeish, T. C.; Pitkeathly, M.; Radford, S. E. *Nature* **1997**, *386*, 259–262.
- (17) Aggeli, A.; Nyrkova, I. A.; Bell, M.; Harding, R.; Carrick, L.; McLeish, T. C.; Semenov, A. N.; Boden, N. *Proc. Natl. Acad. Sci. U.S.A.* **2001**, *98*, 11857–11862.
- (18) Aggeli, A.; Bell, M.; Carrick, L. M.; Fishwick, C. W.; Harding, R.; Mawer, P. J.; Radford, S. E.; Strong, A. E.; Boden, N. *J. Am. Chem. Soc.* **2003**, *125*, 9619–9628.
- (19) Aggeli, A.; Bell, M.; Boden, N.; Carrick, L. M.; Strong, A. E. *Angew. Chem., Int. Ed.* **2003**, *42*, 5603–5606.
- (20) Kayser, V.; Turton, D. A.; Aggeli, A.; Beevers, A.; Reid, G. D.; Beddard, G. S. *J. Am. Chem. Soc.* **2004**, *126*, 336–343.
- (21) Meegan, J. E.; Aggeli, A.; Boden, N.; Brydson, R.; Brown, A. P.; Carrick, L.; Brough, A. R.; Hussain, A.; Ansell, R. J. *Adv. Funct. Mater.* **2004**, *14*, 31–37.
- (22) Schneider, J. P.; Pochan, D. J.; Ozbas, B.; Rajagopal, K.; Pakstis, L.; Kretsinger, J. *J. Am. Chem. Soc.* **2002**, *124*, 15030–15037.
- (23) Pochan, D. J.; Schneider, J. P.; Kretsinger, J.; Ozbas, B.; Rajagopal, K.; Haines, L. *J. Am. Chem. Soc.* **2003**, *125*, 11802–11803.
- (24) Rajagopal, K.; Schneider, J. P. *Curr. Opin. Struct. Biol.* **2004**, *14*, 480–486.
- (25) Zhang, S.; Holmes, T.; Lockshin, C.; Rich, A. *Proc. Natl. Acad. Sci. U.S.A.* **1993**, *90*, 3334–3338.
- (26) Holmes, T. C.; de Lacalle, S.; Su, X.; Liu, G.; Rich, A.; Zhang, S. *Proc. Natl. Acad. Sci. U.S.A.* **2000**, *97*, 6728–6733.
- (27) Zhang, S.; Marini, D. M.; Hwang, W.; Santoso, S. *Curr. Opin. Chem. Biol.* **2002**, *6*, 865–871.
- (28) Semino, C. E.; Kasahara, J.; Hayashi, Y.; Zhang, S. G. *Tissue Eng.* **2004**, *10*, 643–655.
- (29) Choo, D. W.; Schneider, J. P.; Graciani, N. R.; Kelly, J. W. *Macromolecules* **1996**, *29*, 355–366.
- (30) Lashuel, H. A.; Labrenz, S. R.; Woo, L.; Serpell, L. C.; Kelly, J. W. *J. Am. Chem. Soc.* **2000**, *122*, 5262–5277.

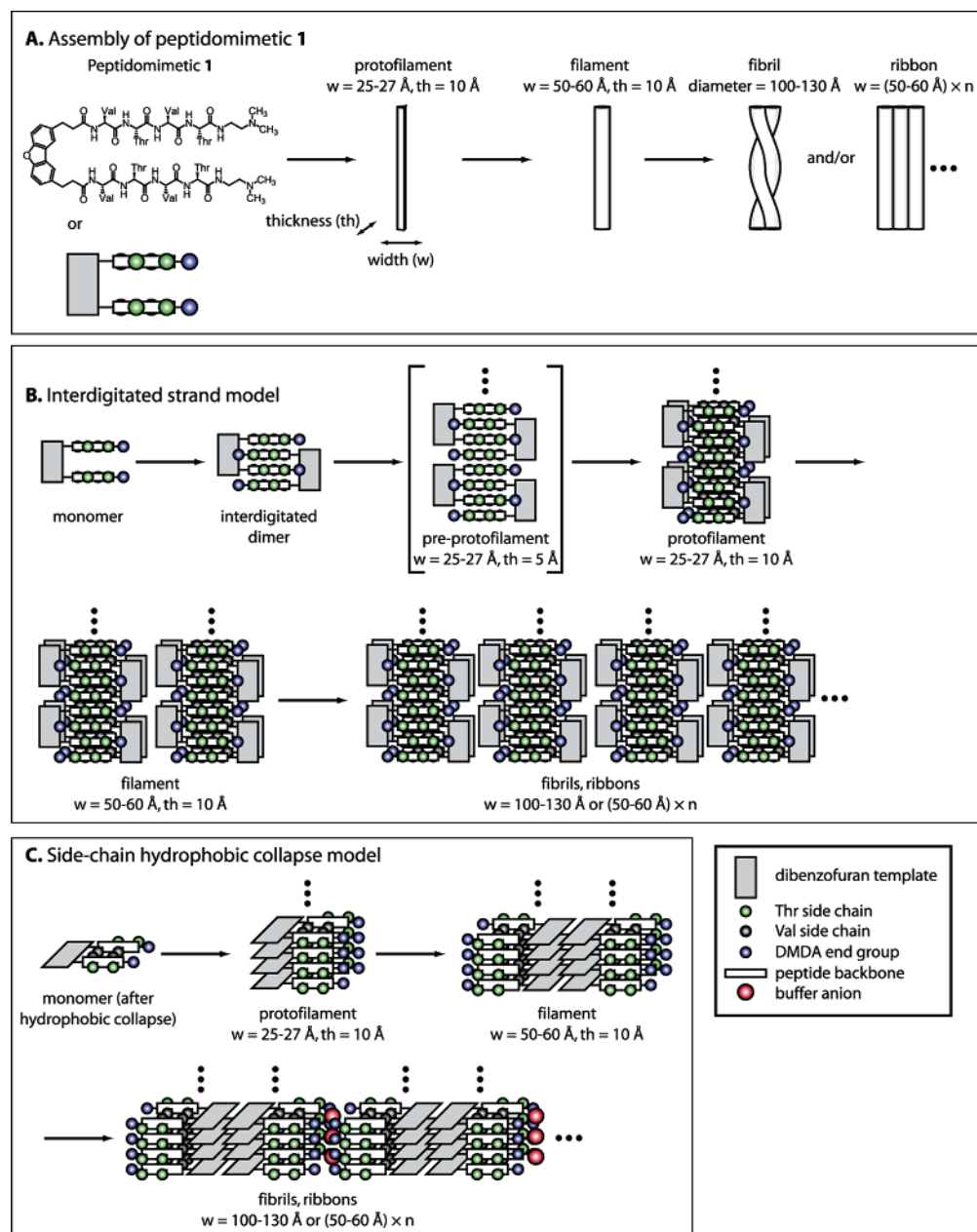


**Figure 1.** (A) Structure of peptidomimetic **1** and the assemblies it forms (protofilaments, filaments, fibrils, and ribbons). The widths ( $w$ ) and thicknesses ( $th$ ) of the assemblies are indicated in the figure. (B) Interdigitated strand model for the assembly of peptidomimetic **1**. The dibenzofuran templates are depicted as gray rectangles. The  $\alpha$ -amino acid side chains are depicted as black (Val) or green (Thr) balls, while the C-terminal DMDA groups are depicted as blue balls. The backbone amides are in the plane of the white rectangles representing the peptide strands; neighboring white rectangles therefore imply intermolecular hydrogen bonding. (C) Side chain hydrophobic collapse model for the assembly of peptidomimetic **1**. The components of the peptidomimetic are represented as in Figure 1B. Buffer anions are depicted as red balls. See text for detailed descriptions of the models.

control over their supramolecular structures and properties. To this end, we have previously synthesized peptidomimetic **1** (Figure 1A) and have carried out a preliminary assessment of the structure of its assemblies.<sup>30</sup>

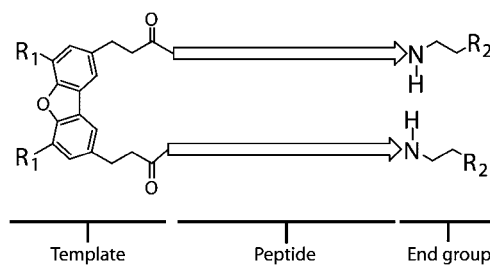
Peptidomimetic **1** consists of two peptide strands attached by their N-termini to propanamide linkers at the 2 and 8 positions of a dibenzofuran substructure. The four residue peptide strands are composed of alternating valine and threonine residues (selected because of their high  $\beta$ -sheet propensities). Peptidomimetic **1** was found to assemble into protofilaments, filaments, fibrils, and ribbons, with the distribution of species depending on the aqueous buffer used (Figure 1A).<sup>30</sup> The dimensions of the assemblies were measured using transmission

electron microscopy (TEM) and atomic force microscopy (AFM). The protofilaments, which were a minor species under all conditions examined, were 25–27 Å wide. The filaments were 50–60 Å wide, and the fibrils and ribbons had widths that were multiples of 50–60 Å. The thicknesses (determined by AFM height measurements) of the protofilaments, fibrils, and ribbons were multiples of 10–11 Å. X-ray fibril diffraction, circular dichroism (CD) spectroscopy, and infrared (IR) spectroscopy revealed that assemblies of **1** had a cross  $\beta$ -sheet structure, in which the peptide strands were oriented perpendicular to the fibril axis. Consistent with this finding, the assemblies bound dyes known to be selective for cross  $\beta$ -sheet structures (thioflavin T and Congo red).<sup>31,32</sup>

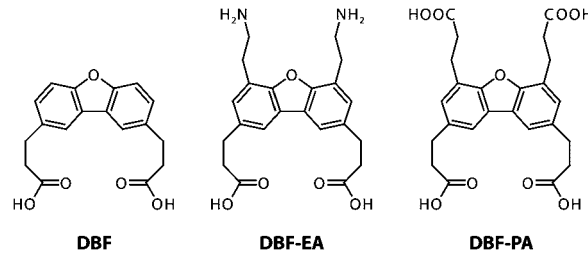
This information was used to infer a structural model for the assemblies formed by **1**, which will be referred to as the “interdigitated strand” model (Figure 1B).<sup>30</sup> The basic unit of the assemblies according to this model is a dimer composed of interdigitated monomers of the peptidomimetic, in which the dibenzofuran substructure acts as a template for intermolecular  $\beta$ -sheet formation. These intermolecularly hydrogen bonded dimers assemble through intermolecular  $\beta$ -sheet formation, in which the hydrogen bonds are collinear with the fibril axis and the side chains are oriented perpendicular to the sheets. This yields a structure that is 25–27 Å wide and 5–6 Å thick, which will be referred to as a pre-protofilament. The alternating Val and Thr side chains are on opposite sides of the structure, creating hydrophobic and hydrophilic faces. Two pre-protofilaments can associate by burying their hydrophobic Val faces, yielding a protofilament that is 25–27 Å wide and 10–11 Å thick, as observed. The protofilaments can then associate laterally along their edges, a process that would be governed by interactions between dibenzofuran substructures (and therefore driven by the hydrophobic effect), to produce 50–60 Å-wide filaments. Further edge-to-edge assembly of the filaments would produce wider structures, such as ribbons and fibrils, with widths that are multiples of 50–60 Å, as observed. In this model, backbone–backbone hydrogen bonding and interstrand side-chain–side-chain hydrophobic interactions drive assembly along the long axis of the assemblies (i.e. the formation of pre-protofilaments), while hydrophobic interactions drive the formation of higher order structures (protofilaments, filaments, fibrils, and ribbons). The interdigitated strand model is consistent with the existing data on assemblies of **1**, but it has a significant weakness: it cannot explain why the observed filaments, fibrils, and ribbons had widths that were multiples of 50–60 Å rather than 25–27 Å. A hypothesis involving “strand swapping” between protofilaments was proposed to rationalize the 50–60 Å repeat.<sup>30</sup>

An alternative structural model, which will be referred to as the “side chain hydrophobic collapse” model (Figure 1C), recently became apparent with the publication of a structural model for  $A\beta$  amyloid fibrils based on solid-state NMR data ( $A\beta$  amyloidogenesis is thought to cause Alzheimer’s disease).<sup>33,34</sup> In this model, the side chains of  $A\beta$  peptides are turned inward on themselves, so that intramolecular interactions are mediated by the side chains, not by hydrogen bonding between peptide amides as would occur if the peptides adopted a  $\beta$ -hairpin conformation. Assembly then occurs by intermolecular backbone–backbone hydrogen bonding to form cross  $\beta$ -sheets. The final assembled cross  $\beta$ -sheet structure is also stabilized by the hydrophobic effect through intermolecular side chain packing. While the analogy between peptidomimetic **1** and  $A\beta$  is imperfect (due to the semirigid spacer that **1** contains), **1** may still assemble like  $A\beta$ . The gap between the strands attached at the 2 and 8 positions of the dibenzofuran template in **1** is large enough to accommodate a conformation analogous to that adopted by  $A\beta$  subunits in amyloid fibrils, in which the Val side chains are turned inward, toward each other (Figure

**Table 1.** Summary of Peptidomimetics Prepared and Their Compositions



peptidomimetic	template (R <sub>1</sub> )	peptide	end group (R <sub>2</sub> )
<b>1</b>	DBF (H)	(ValThr) <sub>2</sub>	N(CH <sub>3</sub> ) <sub>2</sub>
<b>2</b>	DBF (H)	(IleThr) <sub>2</sub>	N(CH <sub>3</sub> ) <sub>2</sub>
<b>3</b>	DBF (H)	(ChaThr) <sub>2</sub>	N(CH <sub>3</sub> ) <sub>2</sub>
<b>4</b>	DBF-EA (CH <sub>2</sub> CH <sub>2</sub> NH <sub>2</sub> )	(ValThr) <sub>2</sub>	N(CH <sub>3</sub> ) <sub>2</sub>
<b>5</b>	DBF-PA (CH <sub>2</sub> CH <sub>2</sub> CO <sub>2</sub> H)	(ValThr) <sub>2</sub>	N(CH <sub>3</sub> ) <sub>2</sub>
<b>6</b>	DBF (H)	(ValThr) <sub>4</sub>	N(CH <sub>3</sub> ) <sub>2</sub>
<b>7</b>	DBF (H)	(ValThr) <sub>2</sub>	N(CH <sub>3</sub> ) <sub>3</sub> <sup>+</sup>



1C). This conformation would be favored by the hydrophobic effect. Peptidomimetic **1** could then self-assemble by intermolecular hydrogen bonding in the direction perpendicular to the strand orientation to yield a protofilament that would be about 25–27 Å wide and 10–11 Å thick. These protofilaments would have the same dimensions as those from the interdigitated strand model; however, in contrast, they would have two different edges: one composed of the hydrophobic dibenzofuran rings and one composed of the hydrophilic C-termini of the peptide strands. The protofilaments would be driven to bury their hydrophobic edges by lateral association in order to minimize their free energy, forming filaments that were 50–60 Å wide. These filaments could then further associate through buffer anion-mediated interactions and/or through hydrogen bonding between the positively charged C-termini to form fibrils and ribbons with widths that were multiples of 50–60 Å. In this model, as in the interdigitated strand model, both backbone–backbone hydrogen bonding and interstrand side-chain–side-chain hydrophobic interactions would drive assembly along the long axis of the cross  $\beta$ -sheet (i.e. the formation of protofilaments), and hydrophobic interactions drive the formation of filaments from protofilaments. In contrast to the interdigitated strand model, the formation of fibrils and ribbons from filaments would be driven by buffer anion-mediated electrostatic and/or hydrogen bonding interactions in the side chain hydrophobic collapse model. According to the latter model, counterions and protonation state of the C-termini would play an important role in higher order assembly. Thus, assembly beyond the filament stage would be highly buffer-dependent.

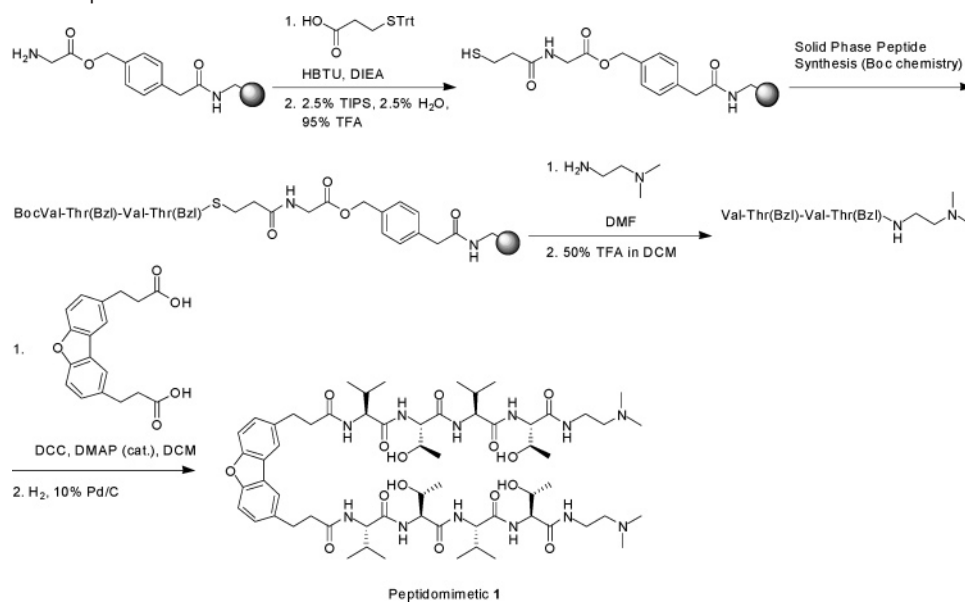
Here, we first describe the design, synthesis, and assembly characteristics of analogues of **1** that have enabled us to determine that **1** likely assembles according to the side chain

(31) Klunk, W. E.; Jacob, R. F.; Mason, R. P. *Methods Enzymol.* **1999**, *309*, 285–305.

(32) LeVine, H., 3rd. *Methods Enzymol.* **1999**, *309*, 274–284.

(33) Petkova, A. T.; Ishii, Y.; Balbach, J. J.; Antzutkin, O. N.; Leapman, R. D.; Delaglio, F.; Tycko, R. *Proc. Natl. Acad. Sci. U.S.A.* **2002**, *99*, 16742–16747.

(34) Tycko, R. *Curr. Opin. Struct. Biol.* **2004**, *14*, 96–103.

**Scheme 1.** Synthesis of Peptidomimetic **1**

hydrophobic collapse model. Then we use this model to design analogues of **1** (Table 1) that form assemblies with predictable dimensions and morphologies.

## Results and Discussion

### Synthesis of Dibenzofuran-Containing Peptidomimetics.

The synthesis of peptidomimetic **1**, shown in Scheme 1, begins with coupling thiopropionic acid to Gly-PAM resin in the presence of HBTU.<sup>35,36</sup> This resin functionalization enables attachment of Thr(Bzl) to the resin as a thioester, which is then elaborated into the BocVal-Thr(Bzl)-Val-Thr(Bzl) peptide by solid-phase peptide synthesis using a Boc/benzyl protection strategy. The peptide was cleaved from the resin by nucleophilic attack of *N,N*-dimethylethylenediamine (DMDA) on the C-terminal thioester, affording the C-terminal DMDA amide. The N-terminal Boc protecting group was removed with trifluoroacetic acid (TFA), yielding the peptide with a free N-terminal amine after neutralization. This otherwise protected peptide was coupled to the dibenzofuran-based template (2,8-dibenzofuran-bis(3-propionic acid)) using DCC and DMAP, affording two amide linkages. The protected peptidomimetic was finally hydrogenated to remove the benzyl groups from the Thr side chains. This synthesis is analogous to that reported previously, except that the thiol-derivatized PAM resin was used instead of Kaiser oxime resin.<sup>30,37–40</sup> The disadvantages of using Kaiser resin were that the coupling of the first residue onto the Kaiser oxime resin was slow and incomplete and that the peptide–resin linkage was not completely stable to repetitive TFA treatments.

### Distinguishing between the Interdigitated Strand and Side Chain Hydrophobic Collapse Assembly Models. The $\beta$ -sheets

in assemblies of **1** should be antiparallel according to the interdigitated strand model, but parallel according to the side chain hydrophobic collapse model. This difference in strand orientation suggests that it could be possible to distinguish between the two models using IR spectroscopy. The IR spectra of assemblies of **1** formed at various pH values have a prominent peak corresponding to the amide I band at  $1629\text{ cm}^{-1}$  with a shoulder at higher wavenumbers.<sup>30</sup> These data are consistent with an infinite antiparallel sheet (for which peaks at  $1630$  and  $1690\text{ cm}^{-1}$  would be expected), but they are also consistent with an infinite parallel sheet (for which peaks at  $1637$  and  $1651\text{ cm}^{-1}$  would be expected).<sup>41</sup> The far-UV CD spectrum of assembled peptidomimetic **1** exhibits a broad minimum at  $215\text{--}220\text{ nm}$ , consistent with a  $\beta$ -sheet structure.<sup>30</sup> However, there is currently no basis for distinguishing parallel from antiparallel cross  $\beta$ -sheet assemblies using CD spectroscopy, due to the paucity of data. Furthermore, CD spectroscopy was unlikely to enable ordered assemblies to be distinguished from amorphous aggregates with high  $\beta$ -sheet content. In addition, because both the hydrogen bonding and the hydrophobic effect drive assembly in both models, even the temperature dependence of the assembly stabilities was unlikely to enable the two models to be distinguished. Because IR and CD spectroscopy and thermal denaturation were all unlikely to provide the necessary information, another means to distinguish between the two models was sought.

The side chains of the residues in peptidomimetic **1** play different roles in the interdigitated strand and side chain hydrophobic collapse models. According to the interdigitated strand model (Figure 1B), the size of the side chains should only affect the thickness of the filaments. In contrast, according to the side chain hydrophobic collapse model (Figure 1C), the size of the side chains should determine whether assemblies are observed at all. Peptidomimetics should not be able to assemble if their side chains are too large to be accommodated within the gap between the peptide strands attached at the 2 and 8 positions of the dibenzofuran template. Therefore, to distinguish between these two models, peptidomimetics **2** and

(35) Hackeng, T. M.; Griffin, J. H.; Dawson, P. E. *Proc. Natl. Acad. Sci. U.S.A.* **1999**, *96*, 10068–10073.

(36) Hackeng, T. M.; Fernandez, J. A.; Dawson, P. E.; Kent, S. B.; Griffin, J. H. *Proc. Natl. Acad. Sci. U.S.A.* **2000**, *97*, 14074–14078.

(37) Degrado, W. F.; Kaiser, E. T. *J. Org. Chem.* **1980**, *45*, 1295–1300.

(38) Degrado, W. F.; Kaiser, E. T. *J. Org. Chem.* **1982**, *47*, 3258–3261.

(39) Pichette, A.; Voyer, N.; Larouche, R.; Meillon, J. C. *Tetrahedron Lett.* **1997**, *38*, 1279–1282.

(40) Mellor, S. L.; Wellings, D. A.; Fehrentz, J.-A.; Paris, M.; Martinez, J.; Ede, N. J.; Bray, A. M.; Evans, D. J.; Bloomberg, G. B. In *Fmoc Solid-Phase Peptide Synthesis: A Practical Approach*; Chan, W. C., White, P. D., Eds.; Oxford University Press: Oxford, U.K., 2000; pp 137–181.

(41) Barth, A.; Zscherp, C. *Q. Rev. Biophys.* **2002**, *35*, 369–430.

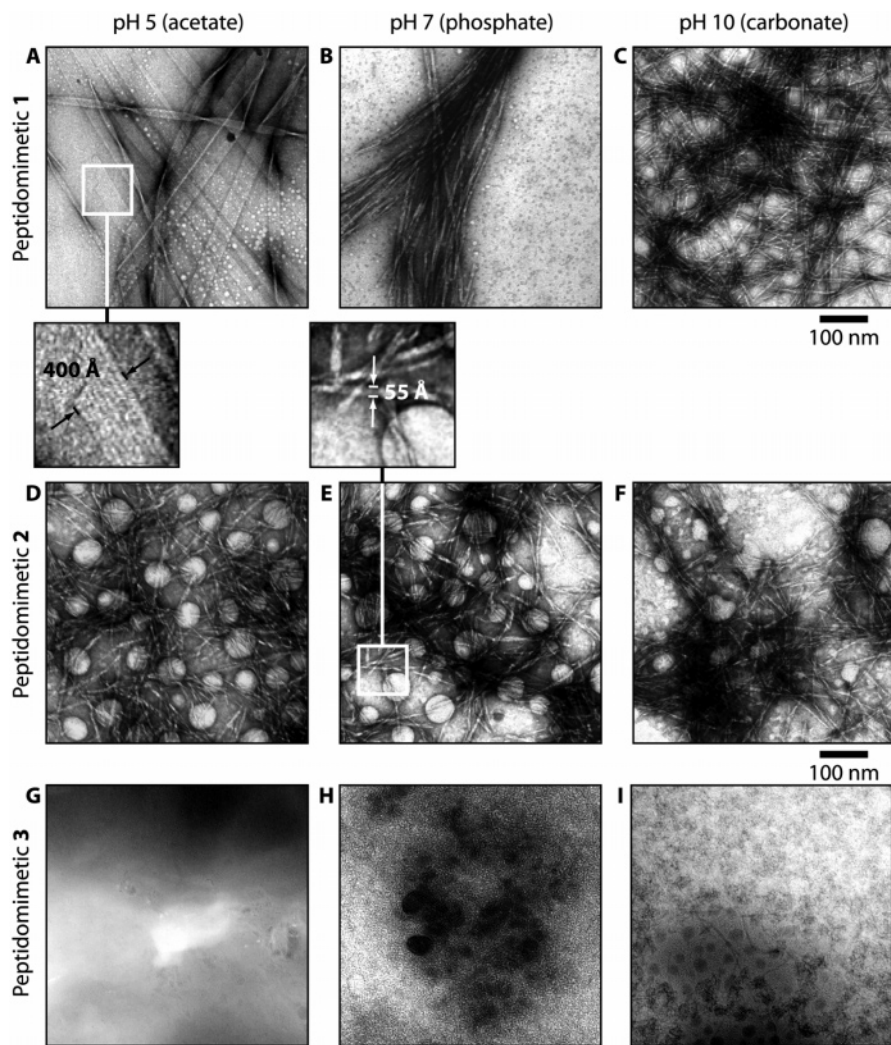


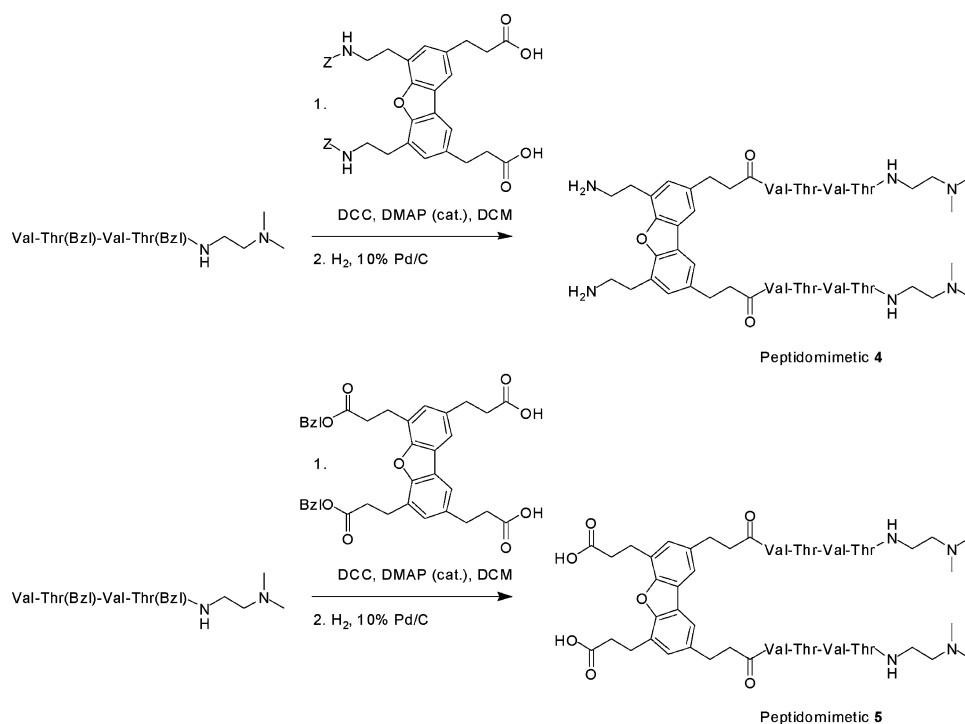
**Figure 2.** (A–C) Negatively stained (uranyl acetate) EM images of peptidomimetic **1** at pH 5 (acetate buffer), pH 7 (phosphate buffer), and pH 10 (carbonate buffer). The expansion for A shows a 3-fold magnification of a 100 nm  $\times$  100 nm patch of the EM image. This patch contains a 400 Å wide ribbon composed of eight filaments. (D–F) EM images of peptidomimetic **2** at pH 5 (acetate buffer), pH 7 (phosphate buffer), and pH 10 (carbonate buffer). The expansion for E shows a 3-fold magnification of a 100 nm  $\times$  100 nm patch of the EM image. This patch contains a 55 Å wide filament. (G–I) EM images of peptidomimetic **3** at pH 5 (acetate buffer), pH 7 (phosphate buffer), and pH 10 (carbonate buffer). The textured appearance of the image shows that the grid is covered by a negatively stained amorphous film derived from peptidomimetic **3** (the grid has a uniform appearance in the absence of sample). No ordered structures are apparent.

**3** (Table 1) were synthesized, in which the Val residues in the peptide strands were replaced by Ile and cyclohexylalanine (Cha), respectively. These peptidomimetics (50  $\mu$ M) were incubated without agitation for 16 h at pH 5 (50 mM sodium acetate buffer, 100 mM NaCl), pH 7 (50 mM sodium phosphate buffer, 100 mM NaCl), or pH 10 (sodium carbonate buffer, 100 mM NaCl), and the assemblies formed were imaged by transmission electron microscopy (TEM).

Peptidomimetic **1** formed ribbons composed of laterally associated filaments at pH 5, consistent with our previous observations (Figure 2A).<sup>30</sup> Some of the ribbons were twisted, likely because of interactions between the ribbons and the EM grid. Whatever the interpretation, it is clear that the periodicity of the twist in the imaged ribbons was highly variable. Peptidomimetic **1** also formed filaments at pH 7 and 10 (Figure 2B,C), and while these filaments had some tendency to co-align (especially at pH 7), they were not tightly associated. In contrast to the variety of morphologies found for **1**, peptidomimetic **2** formed predominantly discrete 50–60 Å wide filaments (the average widths of 12 randomly chosen filaments were  $50 \pm 6$ ,

$60 \pm 12$ , and  $62 \pm 8$  Å at pH 5, 7, and 10, respectively), regardless of the buffer in which assembly was carried out (Figure 2D–F). Fewer than 10% of the species observed were composed of multiple laterally associated filaments. More strikingly, peptidomimetic **3** did not form well-ordered assemblies under any conditions; an amorphous film was observed instead (Figure 2G–I). These results are not consistent with the interdigitated strand model, but can be rationalized using the side chain hydrophobic collapse model as follows. The Ile side chains in **2**, which are only slightly larger than Val side chains, can still be accommodated in the gap between the two peptide strands attached to the dibenzofuran template. Thus, 50–60 Å wide filaments can still form. The space required by the additional methyl group of the Ile side chain, however, forces the peptide strands apart to a degree sufficient to prevent further assembly by the filaments (which requires buffer anion-mediated electrostatic and/or hydrogen bonding interactions between the edges of the filaments; see Figure 1C). The Cha side chains in peptidomimetic **3**, in contrast, are too large to occupy the gap between the peptide strands. Consequently, peptidomimetic **3**

Scheme 2



cannot undergo side chain hydrophobic collapse or self-assembly (since these processes are likely thermodynamically linked). These results compel us to prefer the side chain hydrophobic collapse model to the interdigitated strand model for the structure of peptidomimetic assemblies, a model further scrutinized below. We note, however, that a final determination cannot be made until the structures of the assemblies are studied by a higher resolution method, such as solid-state NMR. It is conceivable that **3** could still assemble by the interdigitated strand model. However, the fact that filamentous assemblies were not observed suggests that this assembly pathway is not energetically favorable in comparison to amorphous aggregate formation, presumably driven by nonspecific hydrophobic interactions.

**Rational Control over Assembly Morphology Using the Side Chain Hydrophobic Collapse Model as a Guide to Peptidomimetic Design: Modification of the Dibenzofuran Template.** The dibenzofuran template, the peptide chains, and the C-termini can all be modified to alter the assembly

characteristics of **1**. For example, placing hydrophilic groups at the 4 and 6 positions (on the periphery) of the dibenzofuran template should reduce the propensity of 25–27 Å wide protofilaments to assemble into 50–60 Å wide filaments (see Figure 1C), since this would remove the hydrophobic driving force for association (i.e. burial of the dibenzofuran-dominated edge of the protofilament). To test this hypothesis, new dibenzofuran templates with either ethylamine or propanoic acid substituents at the 4 and 6 positions were prepared (DBF-EA and DBF-PA, respectively; see the Supporting Information for synthetic details) and incorporated into peptidomimetics **4** and **5** (Scheme 2).

The ethylamine and propanoic acid substructures attached to the dibenzofuran template should make the protofilaments formed by **4** and **5** about 5 Å wider than those formed by **1**. Thus, protofilaments and filaments of **4** and **5** (if formed) are expected to be 30–32 and 55–65 Å wide, respectively. Peptidomimetics **4** and **5** (50 μM) were incubated for 16 h at

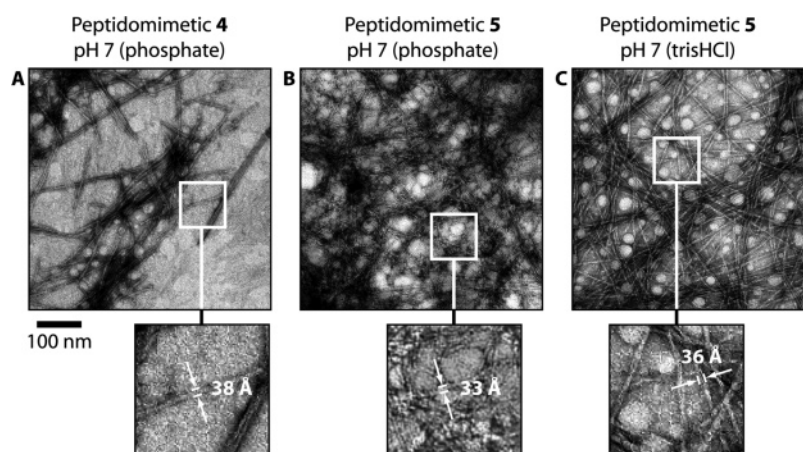


**Figure 3.** (A–C) EM images of peptidomimetics **4** and **5** at pH 7 in phosphate or tris buffer. The expansions are 3-fold magnifications of 100 nm × 100 nm patches of the corresponding EM images. Each expansion contains several typical protofilaments.

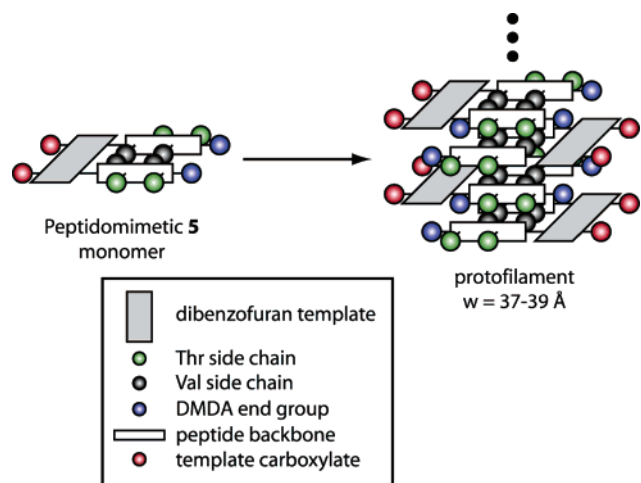


**Figure 4.** Possible assembly mode for peptidomimetic **5**, in which the positions of charged groups alternate from one layer to the next. Protofilaments of peptidomimetic **5** with this structure are expected to be 37–39 Å wide.

pH 5 (50 mM sodium acetate buffer, 100 mM NaCl), pH 7 (50 mM sodium phosphate or tris buffer, 100 mM NaCl), or pH 10 (sodium carbonate buffer, 100 mM NaCl), and the assemblies formed were imaged by TEM.

Peptidomimetic **4** did not self-assemble at pH 5 in acetate buffer, pH 7 in tris buffer, or pH 10 in carbonate buffer, possibly because the 4,6-ethylamine substituents on the dibenzofuran template increased the solubility of the monomer. However, it did assemble at pH 7 in phosphate buffer. The assembly in phosphate buffer, but not in tris buffer at pH 7, is likely due to the presence of a divalent anion ( $\text{HPO}_4^{2-}$ ) in the phosphate buffer. Divalent ions are known to have stronger effects on assembly processes than monovalent ions, presumably through charge neutralization.<sup>42</sup> The assemblies formed were  $38 \pm 5$  Å wide ( $n = 12$ ). This width is much closer to that expected for a protofilament (6 Å too wide) than a filament (17 Å too thin). We therefore assign the observed structures to be protofilaments. Roughly 33% of the discrete species formed by **4** consisted of two or more laterally associated protofilaments. These higher order structures are not like the filaments formed by **1**, because individual protofilaments can be identified within them (i.e. they are not condensed; see the inset to Figure 3A), whereas individual protofilaments cannot be resolved in filaments of **1**. The higher order structures formed by **4** likely occur by  $\text{HPO}_4^{2-}$ -mediated interactions between protofilament edges analogous to those responsible for the formation of ribbons from filaments of **1**, possibly implying that higher order assembly is required in the case of **4** to achieve stabilization. That condensed filaments were not observed among the assemblies formed by **4** supports the hypothesis that modification of the dibenzofuran template can inhibit the formation of filaments from protofilaments. The noncondensed lateral association of protofilaments of **4**, however, suggests that the ethylamine substructure is not ideal for controlling the morphology of the assemblies.

Peptidomimetic **5**, like **4**, did not self-assemble at pH 5 in acetate buffer or at pH 10 in carbonate buffer, but, unlike **4**, it self-assembled at pH 7 in either tris or phosphate buffer to form assemblies that were  $34 \pm 4$  or  $38 \pm 7$  Å wide ( $n = 12$ ; see

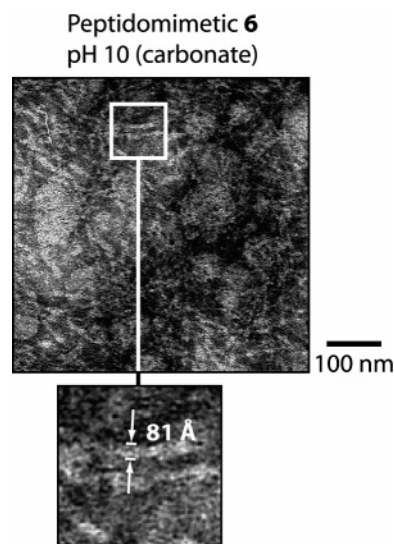


**Figure 5.** EM image of peptidomimetic **6** at pH 10 (carbonate buffer). The expansion is a 3-fold magnification of a 100 nm × 100 nm patch of the EM image, containing several typical filaments.

Figure 3B,C). On the basis of the logic outlined above, these structures were characterized as protofilaments. In contrast to those of **4**, these protofilaments showed no tendency to assemble into higher order structures. The absence of both filaments and looser assemblies of protofilaments demonstrates that assembly widths can be better controlled using the DBF-PA template. The lack of lateral assembly by protofilaments of **5** can be rationalized by noting that, at pH 7, **5** is zwitterionic, whereas **4** bears four positive charges. We speculate that peptidomimetic **5** could assemble as shown in Figure 4, with the template on alternating edges so that the positively and negatively charged functional groups could complement each other. Although the model shown in Figure 4 is speculative, we note that this mode of assembly should reduce the tendency of the protofilaments to self-associate further through anion-mediated and/or hydrogen bonding interactions.

**Control over Assembly Structure by Modification of the Peptide Strands.** According to the side chain hydrophobic collapse model, the width of the protofilaments and filaments (and therefore the periodicity of the ribbons composed of these assemblies) should depend directly on the length of the peptide strands in a given peptidomimetic. Therefore, it should be possible to control the assembly widths by altering the length of the peptide strands. To test this hypothesis, peptidomimetic **6** was prepared (Table 1), which is identical to **1** except that the peptide strands are twice as long (VTVTVTVT). On the basis of the side chain hydrophobic collapse assembly model, protofilaments of **6** should be 13.8 Å wider (39–41 Å wide) than those of **1** and filaments of **6** should be 27.6 Å wider (78–88 Å wide) than those of **1** (typical  $\beta$ -strands are about 3.45 Å long per residue<sup>43</sup>). Peptidomimetic **6** (50  $\mu\text{M}$ ) was incubated for 16 h at pH 5 (50 mM sodium acetate buffer, 100 mM NaCl), pH 7 (50 mM sodium phosphate buffer, 100 mM NaCl), or pH 10 (50 mM sodium carbonate buffer, 100 mM NaCl), and its assemblies were imaged by TEM (Figure 5).

(42) Israelachvili, J. N. *Intermolecular and Surface Forces*, 2nd ed.; Academic Press: London, 1991.

(43) Fraser, R. D. B.; MacRae, T. P. *Conformation in Fibrous Proteins and Related Synthetic Polypeptides*; Academic Press: London, 1973.



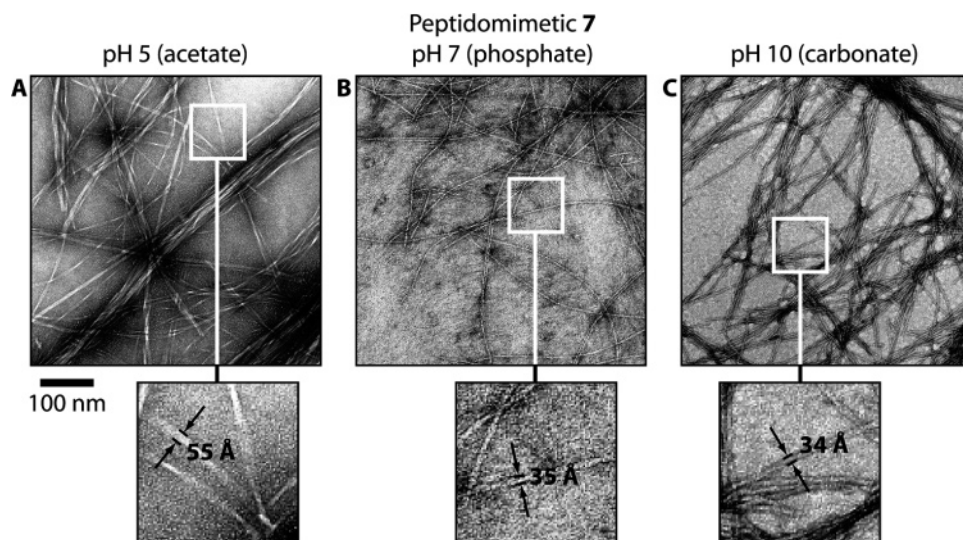
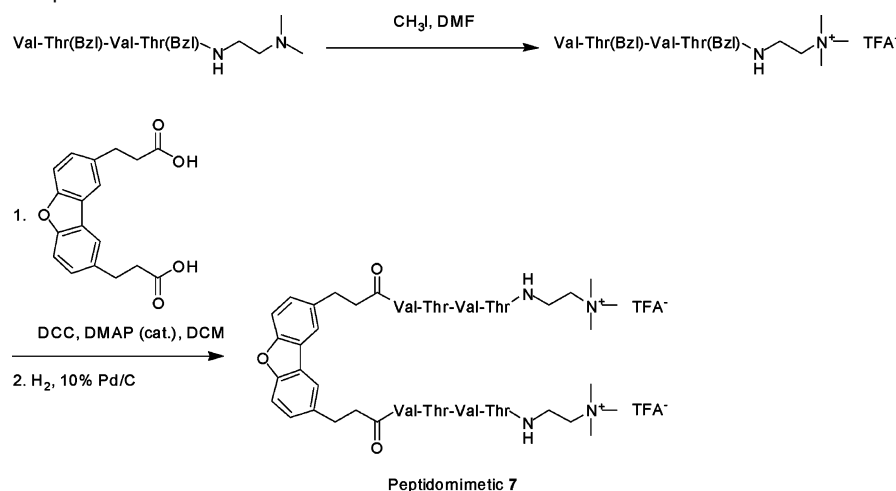


**Figure 6.** (A–C) EM images of peptidomimetic **7** at pH 5 (acetate buffer), pH 7 (phosphate buffer), and pH 10 (carbonate buffer). The expansions are a 3-fold magnification of 100 nm  $\times$  100 nm patches of the corresponding EM images. The expansion for A contains several typical filaments, while those for B and C contain several typical protofilaments.

**Scheme 3.** Synthesis of Peptidomimetic **7**



Peptidomimetic **6** yielded superaggregates of filamentous assemblies at pH 5 and 7 (data not shown), in which the widths of individual structures were ill-defined and therefore could not be measured. However, individual assemblies formed by peptidomimetic **6** could be distinguished at pH 10. These assemblies were  $88 \pm 8$  Å wide ( $n = 12$ ), or roughly 30 Å wider than filaments of **1**, at pH 10. This increase in width is consistent with the side chain hydrophobic collapse model, but it should be noted that this peptidomimetic appears to afford a more heterogeneous distribution of assemblies than the others.

**Control over Assembly Parameters by Modification of the C-Termini.** According to the side chain hydrophobic collapse model (Figure 1C), anion-mediated electrostatic and/or hydrogen bonding interactions between C-terminal DMDA groups on **1** control the lateral assembly of filaments to form structures wider than filaments (fibrils and ribbons). Altering the properties of the C-terminus should therefore alter the ability of the filaments to form fibrils and ribbons. To test this hypothesis, peptidomimetic **7**, in which the DMDA group was replaced by the permanently positively charged *N,N,N*-trimethylethylenediamine moiety, was prepared (Scheme 3).

Peptidomimetic **7** ( $50 \mu\text{M}$ ) was incubated for 16 h at pH 5 (50 mM sodium acetate buffer, 100 mM NaCl), pH 7 (50 mM sodium phosphate buffer, 100 mM NaCl), or pH 10 (50 mM sodium carbonate buffer, 100 mM NaCl), and the assemblies formed were imaged by TEM (Figure 6).

Peptidomimetic **7** self-assembled at pH 5, forming assemblies with an average width of  $61 \pm 6$  Å ( $n = 12$ ), consistent with the width expected for filaments (Figure 6A). These filaments had some tendency to co-align to form noncondensed associated higher order structures—ribbons were observed in some samples (data not shown). In contrast to its behavior at pH 5, peptidomimetic **7** formed assemblies with widths of  $37 \pm 4$  and  $38 \pm 4$  Å ( $n = 12$  each) at pH 7 and 10, respectively, consistent with the width of a protofilament. This unexpected result can be rationalized by proposing that protofilaments of **7** have an internal structure similar to that proposed for protofilaments of **5** (see Figure 4), in which the dibenzofuran template is found on alternating edges of the protofilament. Peptidomimetic **7** may be driven to adopt this structure to decrease the charge density at the protofilament edges. We speculate that the high charge densities in assemblies formed by **1** may perturb the  $pK_a$  values

of the DMDA groups, causing them to be partially deprotonated at pH 7 and completely deprotonated at pH 10. This would enable peptidomimetic **1** to form the assemblies depicted in Figure 1C at pH 7 and 10, but, because the charge on peptidomimetic **7** cannot be removed, peptidomimetic **7** would have to assemble as shown in Figure 4. It is conceivable that each of these two modes of assembly could be observed with a single peptidomimetic under different solution conditions.

### Conclusions

The assembly of peptidomimetic **1** and its analogues is best described by the side chain hydrophobic collapse model illustrated in Figure 1C. This structural model provided a rich variety of approaches by which the assembly morphology of this class of peptidomimetics could be rationally altered. Increasing the hydrophilicity of the dibenzofuran template with propionic acid moieties at the 4 and 6 positions can arrest the assembly process at the protofilament stage. The assembly process at pH 5 can be made to favor filaments by changing the C-terminus from a DMDA to a TMDA group, but this unexpectedly yields protofilaments at higher pH values. The

assembly process at pH 7 and 10 can be more effectively and generally halted at the filament stage by exchanging the Val residues in the strands for Ile residues. Finally, greatly increasing the size of the  $\alpha$ -amino acid side chains can altogether block ordered hydrophobic collapse and the linked assembly process. We hope that this work will encourage the development of analogous, rationally controllable  $\beta$ -sheet assemblies with desirable and designable properties.

**Acknowledgment.** We gratefully acknowledge financial support from the NIH (Grant GM 51105), the Skaggs Institute for Chemical Biology, the Lita Annenberg Hazen Foundation, and a Norton B. Gilula Fellowship (S.D.). We thank Dr. Theresa Fassel for a helpful discussion.

**Supporting Information Available:** All experimental details, including syntheses of the modified dibenzofuran templates DBF-EA and DBF-PA (PDF). This material is available free of charge via the Internet at <http://pubs.acs.org>.

JA050558C